



Multifunctional superhydrophobic composite films from a synergistic self-organization process†

Ming Fang ^a, Zhiyong Tang ^b, Hongbin Lu ^{*a} and Steven Nutt ^c

^aThe Key Laboratory of Molecular Engineering of Polymers of Ministry of Education, and Department of Macromolecular Science, Fudan University, 220 Handan Road, Shanghai, 200433, China.

^bNanomaterials, National Center for Nanoscience and Technology, No. 11, Beiyitiao, Zhongguanchun, Beijing, 100190, China

^cDepartment of Chemical Engineering and Materials Science, University of Southern California, Los Angeles, CA 90089-0241, USA

*E-mail: hongbinlu@fudan.edu.cn; Fax: + 86-21-5566 4589; Tel: + 86-21-5566 4589hongbinl@fudan.edu.cn

Abstract: A synergistic self-organization method was proposed to prepare multifunctional superhydrophobic composite films, which combined well-exfoliated graphene nanosheets (GNs) with a conjugate polymer (poly(3-hexyl thiophene), P3HT) through a simple solution-deposition process. The composite film can be rapidly prepared on various substrates; typically only a few minutes were necessary when the P3HTGN suspension was coated on a metal mesh. The 35 wt% P3HT composite film is superhydrophobic with a contact angle of 159.2°, an electrical conductivity up to 6560 S m⁻¹ and specific electromagnetic interference shielding effectiveness (43.7 dB cm³ g⁻¹) four times greater than solid copper. It has a porous structure with the bulk density of 0.76 g cm⁻³, separation efficiency of over 98% for the n-octane/water mixtures in volume ratios of 1: 1–1: 15, and good environmental stability with a capacity to endure thermal treatment at 200 °C and organic solvents such as methanol, acetone and DMF etc. This synergistic self-organization method was also applied to prepare superhydrophobic P3HTmontmorillonite (MMT) composite films with a contact angle of 161° and a high adhesion capacity to water droplets, proving a versatile method in fabricating functional superhydrophobic films suited to practical applications.

Please cite this article as: H. Lu, and M. Fang, Z. Tang, and S. Nutt, “**Multifunctional Superhydrophobic Composite Films from a Synergistic Self-Organization Process**” J. Mater. Chem. 22 (2012) 109-114. DOI: <http://dx.doi.org/10.1039/C1JM13213J>



1. Introduction

Superhydrophobic surfaces with water contact angles greater than 150° and low contact angle hysteresis are important for applications that include fluid transportation, self-cleaning, sensors, environmental remediation, and solar cells.¹⁻⁷ These superhydrophobic surfaces will become particularly useful when the ease and control in constructing hierarchical multiscale structures are combined with desired functionalities.⁸⁻¹⁰ Recent work has demonstrated that different functionalities can be integrated in artificial superhydrophobic films, including selective absorption for liquids,⁴ stimuli-responded switching between superhydrophilicity and superhydrophobicity,¹¹ self-healing after damage,¹² transparency and electrical conductivity.^{13,14} However, practical industrial applications typically require simplified low-cost fabrication procedures and robust environmental stability, besides superior functionality.¹⁵⁻¹⁷ To meet such requirements, alternative materials and methods for multifunctional materials design are desired. Graphene is well-suited to this task, providing 2-dimensional building blocks with unusual properties¹⁸ that are readily available from an abundant source (natural graphite). Although multiple potential applications based on graphene have been demonstrated, such as transistors,¹⁹ supercapacitors²⁰ and nanocomposites,²¹⁻²⁴ construction of functional superhydrophobic graphene films remains unexplored.

Here we show that such functional superhydrophobic films can be produced using well-exfoliated graphene nanosheets (GNs) and a conjugate polymer through a simple solution deposition technique. The interaction with non-solvents drives polymer chains to deposit spontaneously onto the GN surface (producing nanoscale roughness), which subsequently result in irregular stacking of GNs (microscale roughness) after removal of solvents. The resulting composite films are porous,



lightweight, environmentally stable, and exhibiting excellent oil– water separation efficiency. They have electrical conductivities of over 6500 S m^{-1} and specific electromagnetic interference shielding effectiveness four times greater than solid copper. We also reveal that the synergistic self-organization approach presented here may be applied to other composite systems, proving a cost-effective, industrially viable route to the fabrication of functional superhydrophobic films suited to practical applications.

2. Experimental section

2.1 Materials

Exfoliated GNs were prepared using the common commercial expandable graphite (EG) following the method proposed by Dai et. al.^{21b} The electron diffraction and X-ray photoelectron spectrum (XPS) indicate that the GNs obtained retain well the perfectness of grapheme crystal structures. Regioregular Poly(3-hexyl thiophene) (P3HT) was synthesized following the Grignard metathesis method.^{21c} ¹H-NMR and gel permeation chromatography (GPC) reveal that the obtained P3HT is regioregular (98.5%); the number average molecular weight and polydispersity index are 21,000 and 1.76, respectively. Tetrahydrofuran, N, N-dimethyl formamide (DMF) and ether were purified prior to use. Other reagents were used as received. The detailed description was provided in the Supplementary Information.[†]

2.2 Preparation of superhydrophobic P3HT composite films

P3HT was dissolved in chloroform to form a homogeneous yellow solution (10 mg mL^{-1}) to which a certain amount of GNs were added. Sonication was used to prompt dispersion of GNs in the above solution. Methanol was added dropwise to the above suspension. After sonication (~5 min), the suspension obtained was dropcast on glass or other substrates such as filter papers, metal meshes



and poly(ethylene terephthalate) films. The obtained films were dried at room temperature or using a blow dryer. Other poor solvents including hexane, DMF and acetone were also examined in order to evaluate the effect of the synergistic self-organization process on the superhydrophobicity of composite films. Among these poor solvents, the use of DMF requires a drying condition of around 70 °C. Montmorillonite/P3HT composite films were prepared following the same procedure.

2.3 Characterization

Microscopy. Transmission electron microscope (TEM, JEOL-1230) was used to observe the morphology of as-prepared GNs that deposited on standard copper grids. The selected area electron diffraction allows for evaluation of the perfectness of graphene crystal structures. Scanning electron microscope (Philips XL30 FEG FE-SEM) was employed to observe the microscale rough surface of the composite films with different P3HT contents. Atomic force microscope (Nanoscope IV system, Digital Instruments, Santa Barbara CA) was used to evaluate the nanoscale roughness of P3HT composite films, including those samples suffering from thermal treatments. The observation was performed in tapping mode at room temperature.

Spectroscopy. XPS was used to characterize the amount of C–O species on exfoliated GNs and the surface component of P3HT and composite films. The measurements were conducted on a RBD upgraded PHI-5000C ESCA system (Perkin Elmer) with a Mg-K α radiation ($h\nu = 1253.6$ eV) or a Al K α radiation ($h\nu = 1486.6$ eV). The X-ray anode was run at 250W and the high voltage was kept at 14.0 kV with a detection angle at 54°. The pass energy was fixed at 46.95 eV to ensure sufficient resolution and sensitivity. The base pressure of the analyzer chamber was $\sim 5 \times 10^{-8}$ Pa. X-ray diffraction (XRD) was used to characterize the crystal structure of GNs, graphite, P3HT and composite films. The measurements were conducted on a Rigaku D/max- $\gamma\beta$ diffractometer with Cu-



K α radiation ($\lambda = 0.154$ nm) at a scanning rate $0.02^\circ/\text{s}$ and an angle range from 3 to 80° . UV-vis spectra of the P3HT-GN suspensions were recorded on a NEXUS 670 spectrometer, which allows for evaluating the effect of poor or non-solvent addition on the π - π stacking occurred during the self-organization. The further description for these UV-vis measurements is presented in the Supplementary Information.

Contact angle (CA). Dataphysics OCA20 contact-angle system was used to characterize the wetting behavior of composite films at ambient temperature. The CA value was obtained by averaging five measuring results at different positions of the same sample. A constant volume of water (3 mL) was used in all measurements and the corresponding contact angles were obtained by ellipse fitting with the SEC software.

Electrical conductivity and electromagnetic interference shielding (EMI) properties. The electrical conductivity of the composite films was measured at room temperature with a standard four-probe method, using a Keithley 196 system DMM Digital Multimeter, and an Advantest R1642 programmable DC voltage/current generator as the current source. A portable digital multimeter Victor VC9807A+ was also used to measure the electrical resistance of the composite film in order to compare the difference between the composite film and metal (an AFM sample stage). All EMI measurements were conducted over the frequency range of 8–12 GHz using a WILTRON 54169A Scalar Measurement System in accordance to the standard procedure. The size of samples is $22.8 \times 10.1 \times 2$ mm³. The total EMI effectiveness (SE_{total} in decibel) was recorded in terms of the contributions from reflection (SE_{R}) and absorbance (SE_{A}), that is, $SE_{\text{total}} = SE_{\text{R}} + SE_{\text{A}}$.

Thermal properties. Differential scanning calorimetry (DSC Q2000, TA) was used to characterize the melting behaviour of P3HT at a heating rate 10 °C



min^{-1} in nitrogen. Thermogravimetric analysis (TGA Pyris 1, Perkin Elmer) was employed to study the thermal stability of pristine P3HT and composite films at a heating rate $20\text{ }^{\circ}\text{C min}^{-1}$ in nitrogen.

Oil–water separation efficiency. GNs (65 wt% relative to P3HT) were dispersed in chloroform solution containing 10 mg mL^{-1} P3HT. After adding 15 vol% methanol (relative to chloroform), the suspension was coated on an iron mesh and dried with an ordinary blow dryer. This mesh was used to separate the oil (n-octane)-water mixtures with different ratios. The separation efficiency $E_{O/W}$ of oil–water mixtures was calculated in accordance with $E_{O/W} = \text{water weight after separation} / \text{water weight before separation}$

Environmental stability. The composite films were first immersed for 30 min in hot water and organic solvents including methanol, acetone, DMF and hexane. After drying, the measured water contact angles were used to evaluate the effect of these solvents on the superhydrophobicity of the composite films. Subsequently, these films suffered from thermal treatments in an oven (air atmosphere) preset at different temperatures for the same time. Thermal treatment of the composite films in inert atmosphere was conducted in TGA. AFM, XRD and CA measurements were used to characterize the changes in structure and hydrophobicity of composite films.

3. Results and discussion

The wetting behavior of a film is primarily affected by its chemical components (surface energy) and surface roughness.¹⁶ For a given system, the surface roughness plays a critical role in tuning its wettability. Roughness usually gives rise to some amplification effect of wetting behaviours, as described by the Wenzel/Cassie model.¹⁷ A hydrophobic surface will become more hydrophobic and even superhydrophobic when the surface roughness increases. Reduced GNs have exceptional electrical and thermal properties but they are generally hydrophobic. To achieve the



superhydrophobicity of GN-based films, their surface roughness needs to be improved through appropriate approaches.

We prepare functional superhydrophobic composite films using a solubility-driven synergistic self-organization process. Poly(3-hexyl thiophene) (P3HT, regioregularity 98.5%, number average molecular weight 21,000) was used to create hierarchical nanoscale surface roughness (50–300 nm) on exfoliated GNs (see Supplementary Information, Fig. S1–S4[†]). P3HT was first dissolved in chloroform to form a homogeneous solution (10 mg mL⁻¹). GNs were subsequently dispersed in the above solution using sonication, yielding a tan-colored suspension. The addition of methanol triggered P3HT aggregation and rapid deposition onto the GN surface, as shown in Fig. 1a. The resulting suspension can be readily coated on various substrates by simple drop-coating to create functional superhydrophobic films with a water contact angle of 159.2°.

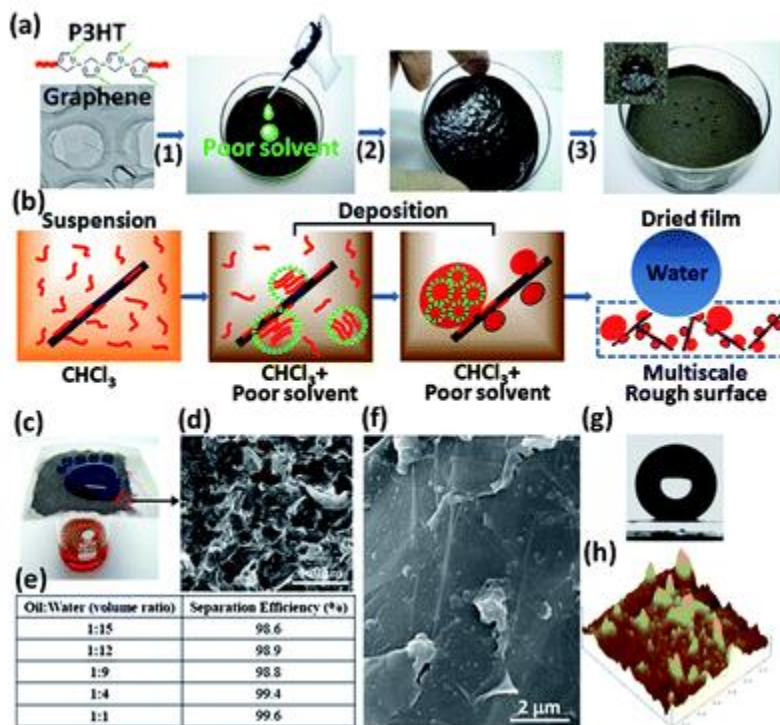


Fig. 1 (a) The fabrication process for superhydrophobic composite films. (1) P3HT and GNs are mixed to form a tan-colored suspension; (2) gradual addition of a poor solvent/nonsolvent induces aggregate



formation in solution and on GNs, as well as occurrence of gelation after partial removal of solvents; (3) a dried composite film in a petri dish exhibits superhydrophobicity (denoted by spherical water droplets). (b) Synergistic self-organization mechanism for rapid fabrication of superhydrophobic GN-P3HT composite films. (c) The GN-P3HT composite film coated on a metal mesh was used to separate octane (red) and water (dyed with methyl blue, above the mesh). (d) SEM image showing that the GN-P3HT composite film coated on the metal mesh is porous (as denoted by red dash lines), which allows octane to flow through; the scale is 100 μm . (e) Separation efficiency of the GN-P3HT composite film for different oil–water mixtures. (f) SEM image of the 35 wt% P3HT composite film surface. (g) The 35 wt% P3HT composite film shows a water contact angle of 159.2°. (h) AFM image of the 35 wt% P3HT composite film shows that a large amount of small protrusions (50–70 nm in lateral sizes and 5–50 nm in height) and large aggregates (200–300 nm in lateral sizes and 20–40 nm in height).

The self-organization of P3HT during solution-deposition involves homogeneous nucleation of P3HT in solution and heterogeneous nucleation on the GN surface, see Fig. 1b. In a methanol-free P3HT-GN suspension, some polymer chains attach to the GN surface through π – π interactions, preventing GNs from aggregation and improving their dispersion stability.²⁵ The addition of methanol induces the formation of P3HT aggregates in solution and on the GN surface, thereby minimizing unfavourable interactions with solvent molecules.²⁶ GNs provide a large number of nucleation sites and diminish the formation probability of gel-like P3HT agglomerates in solution. Simultaneously, the P3HT nanoparticles deposited on GNs inhibit the re-aggregation of GNs during drying. Such synergism leads to the rapid formation of multiscale rough surfaces, which reduces the dependence on drying conditions and greatly simplifying the procedure for fabrication of superhydrophobic films. For instance, such films can be prepared on metal meshes in a few minutes using an ordinary blow dryer (see Video S1†). Furthermore, because of their porous feature (Fig. 1d), these films also afford an excellent oil–water separation capacity. When coated on an iron mesh, for example, the 35 wt% P3HT composite film achieved separation efficiencies of over 98% for octane-water mixtures with volume ratios from 1 : 1 to 1 : 15, (see Fig. 1c,e, Video S1†).

The synergistic self-organization of P3HT and GNs in suspensions is evident in UV-vis spectra and XRD. The characteristic absorption of P3HT in chloroform is the intra-chain π –



π^* transition that appears at ~ 450 nm; however, after adding methanol to the suspension, a notable red shift occurs, resulting in two new bands at 560 and 605 nm, indicating that some of the P3HT chains were organized in a parallel stacking conformation (Fig. 2a).^{26,27} XRD patterns indicate that GNs promoted the ordered stacking of P3HT in the composite film (Fig. 2b). Compared to the pristine P3HT film, both the stronger $\{100\}$ diffraction peak and the smaller interlayer spacing suggest more perfect stacking of P3HT crystals on GNs, while the notable weakening of the graphite peak at $2\theta = 26.8^\circ$ reflects the effectiveness of the ordered P3HT stacking in inhibiting aggregation of GNs. The SEM and AFM images of the 35 wt% P3HT composite film in Fig. 1f, h shows that numerous protrusions (50–70 nm in lateral sizes and 5–50 nm in height) and aggregates (200–300 nm in lateral sizes and 20–40 nm in height) are situated on the GN surface, along with an average roughness $R_a = 3.2$ nm. This constructs a superhydrophobic surface with a contact angle of 159.2° (Fig. 1g).

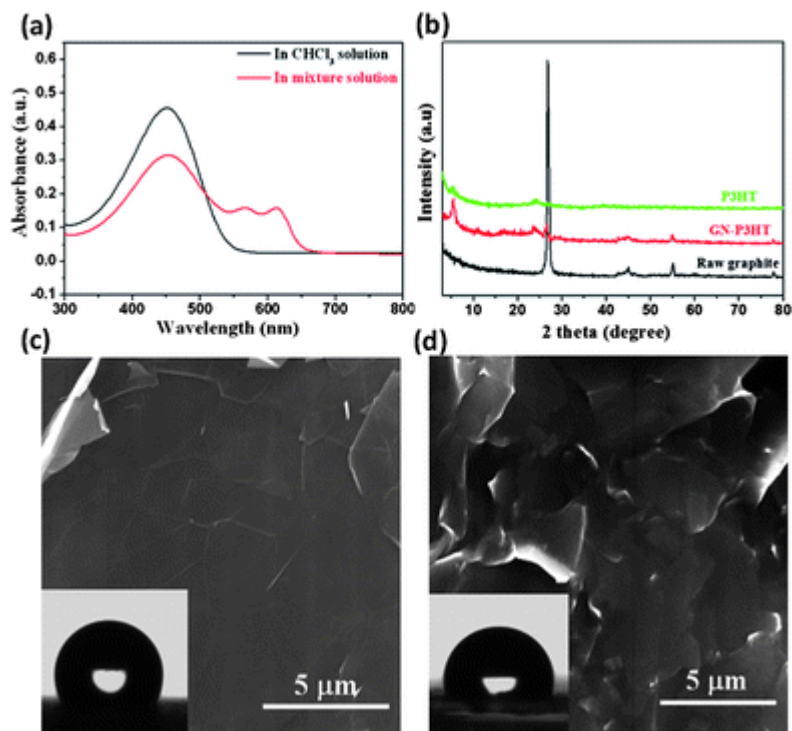




Fig. 2 (a) UV-vis absorption spectra of the GN-P3HT suspensions before (black line) and after (red line) adding methanol. (b) XRD curves of raw graphite powder, P3HT and 35 wt% P3HT composite films. (c) SEM image of the P3HT-free GN film formed by filtration shows a smooth surface with a water contact angle of 115°. (d) SEM image of the 35 wt% P3HT composite film obtained by direct volatilizing chloroform (without adding methanol) displays no nanoscale protrusions on the GNs, with a water contact angle of 98.5°.

Two factors might significantly affect the wetting behavior of GN composite films, that is, the content of P3HT and the type of non-solvents used during deposition. Direct deposition of GNs by volatilization did not produce a superhydrophobic film on the substrate – the resulting film revealed a contact angle of only 115°, indicating lack of nanoscale roughness (Fig.2c). In the absence of non-solvent, the GN-P3HT suspension produced a hydrophobic surface with a contact angle of 98.5° (Fig. 2d), similar to that of the pristine P3HT film (91°). It is apparent that a contracted P3HT conformation is necessary for forming nanoscale roughness. In addition, reducing the concentration of P3HT markedly diminished the hydrophobicity of the resulting films due to a decrease in the size of nanoscale protrusions on GNs. For the 10 wt% P3HT composite film, the average protrusion size decreased to ~60 nm from ~200 nm in the 35 wt% P3HT film, and the corresponding contact angle decreased to 142°. When the P3HT concentration was reduced to 5 wt%, the protrusion size further decreased to ~24 nm, and the corresponding contact angle dropped to 124° (see Fig. S5–S7[†]). The effect of adding non-solvents, including acetone, dimethyl formamide (DMF) and hexane, on the deposition process of P3HT on GNs was also examined. Additions of both acetone and DMF (but not hexane) resulted in the formation of superhydrophobic composite surfaces, with contact angles slightly lower than those produced by adding methanol. This reflects the difference in driving force of non-solvents for the ordered stacking of P3HT chains (see Supporting Information and Fig. S8–S10[†]).



The environmental stability of functional films is of vital importance for practical applications. Fig. 3a presents the thermogravimetric results of the pristine P3HT and 35 wt% composite films in nitrogen. The composite film shows a ~ 40 °C increase in the initial decomposition temperature compared to the pristine P3HT. The improved thermal stability primarily arises from the effect of GNs, which inhibit the release of volatile components.²⁸ To further evaluate the thermal stability, composite films deposited on iron meshes were annealed at different temperatures, the changes in structure and hydrophobicity were then examined. Generally, when annealing below the melting temperature of P3HT (232 °C, Fig. S11–12[†]), the composite film showed no significant changes in both surface structure and water contact angle. Even when annealing for 30 min at 400 °C in nitrogen, only a slight decrease in contact angle (from 157.2 to 156.5°) and an increase in tilt angle (from 8.5° to 13°) were observed; the latter indicates an increase in adhesion to water droplets (Fig. 3b). However, a 30-min annealing at 600 °C in nitrogen caused a significant change in wetting behavior, transforming the composite film into a highly adhesive surface. Nevertheless, the films retained moderate hydrophobicity (contact angle 130°). Microscopic observation (Fig. 3c, d) and diffraction results (Fig. S12b[†]) indicated that the decreased hydrophobicity and increased surface adhesion are associated with loss of surface roughness and the capillary effect of irregular stacking of GNs. By comparing the morphology of P3HT nanoparticles on GNs surface, it is clear that the annealing at 400 °C reduced the nanoscale roughness of the composite film to a certain extent while the annealing at 600 °C nearly completely removed the polymer nanoparticles deposited on GN surfaces, except some smaller residual debris. The roughness analysis for these AFM images shows that the average roughness R_a of the GN surface reduces from the original 3.2 nm (Fig. 1h) to 2.5 nm (Fig. 3c) and 0.66 nm (Fig. 3d), respectively.

Please cite this article as: H. Lu, and M. Fang, Z. Tang, and S. Nutt, “**Multifunctional Superhydrophobic Composite Films from a Synergistic Self-Organization Process**” *J. Mater. Chem.* 22 (2012) 109-114. DOI: <http://dx.doi.org/10.1039/C1JM13213J>

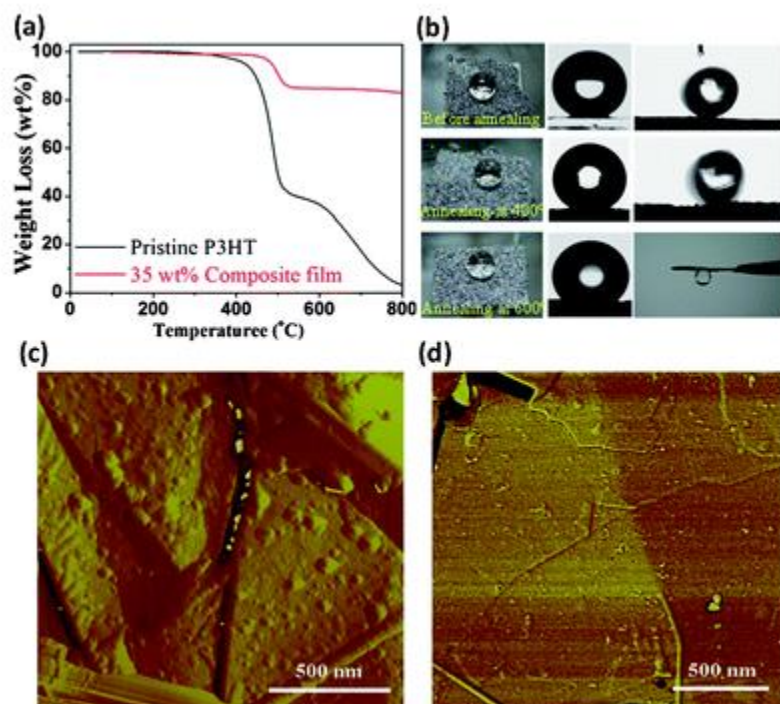


Fig. 3 (a) Thermogravimetric curves of the pristine P3HT film and 35 wt% P3HT composite film in nitrogen. (b) A dried 35 wt% P3HT composite film (left) shows a contact angle of 159.2° (center in the first row) and a tilt angle of 8.5° (right); after annealing at 400°C for 30 min the composite film shows a contact angle of 156.5° and a tilt angle of 13° ; after annealing at 600°C for 30 min the composite film yields a contact angle of 130° and a tilt angle of 180° , namely, strong adhesion to a water droplet. The AFM morphologies of P3HT protrusions on the GN surface after annealing (in nitrogen) under different conditions: (c) 400°C , 30 min, and (d) 600°C , 30 min.

Given the extraordinary properties of GNs, some desired functionalities can be imparted. As shown in Fig. 4a and Video S2,[†] the 35 wt% P3HT composite film exhibits a resistance of only $\sim 27\ \Omega$, roughly 50 times greater than that of a highly conductive metal AFM sample stage ($0.54\ \Omega$). Additional measurements of electrical conductivity for composite films with different P3HT contents were subsequently conducted following the standard four-probe method. For the P3HT-free GN film, it reveals an electrical conductivity of $10780\ \text{S m}^{-1}$ (Fig. 4a), reflecting the highly perfect crystal structure in exfoliated GNs and agreeing with the XPS results (Fig. S1c[†]). The deposition of P3HT inhibits charge transport in the composite film due to the reduced contact probability between



GNs; for example, the 5 wt% P3HT composite film shows a reduction in conductivity of $\sim 1300 \text{ S m}^{-1}$. Nevertheless, the superhydrophobic composite with 35 wt% P3HT retains a quite high electrical conductivity (6560 S m^{-1}). Similar excellent properties have recently been reported by Cao *et al.*, who adopted a facile and low-cost vacuum filtration technique to prepare mechanically strong and highly conductive superhydrophobic carbon nanotube (CNT) composite films.¹⁴ By comparison, however, the superhydrophobic GN-P3HT film can be prepared in a more flexible manner (in a few minutes and with a simple drop-casting method) and furthermore reveals a higher electrical conductivity.

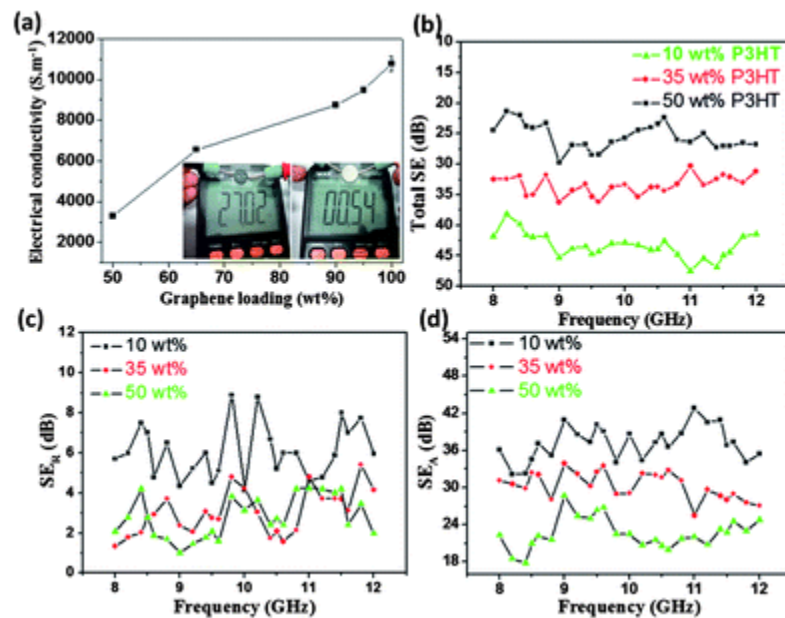


Fig. 4 (a) Electrical conductivities of GN-P3HT composite films change as a function of GN contents; the inset show the electrical resistance of the GN-35 wt% P3HT composite film (left) obtained using a digital multi-meter (Victor VC9807A+) and for comparison, the result of a metal sample stage of an AFM instrument is also shown (right). (b) The effect of P3HT content on the total shielding efficiencies of GN-P3HT composite films. (c) Reflection of composite films to the electromagnetic input (SE_R). (d) Absorbance of composite films to the electromagnetic input (SE_A).

High electrical conductivity makes the superhydrophobic films a promising candidate for use as superhydrophobic EMI shielding materials. Fig. 4b–d show the influence of P3HT content on the

total electromagnetic shielding. All measurements were conducted with a sample size of 22.8×10.1

Please cite this article as: H. Lu, and M. Fang, Z. Tang, and S. Nutt, "Multifunctional Superhydrophobic Composite Films from a Synergistic Self-Organization Process" *J. Mater. Chem.* 22 (2012) 109-114. DOI: <http://dx.doi.org/10.1039/C1JM13213J>



$\times 2 \text{ mm}^3$ in the frequency range of 8–12 GHz, following the standard industrial test procedure (Fig. S13[†]). Increasing the P3HT content in composite films reduced the SE_{total} (Fig. 4b), which agrees with electrical conductivity measurements. For example, the 35 wt% P3HT composite film showed a SE_{total} value at 10 GHz of 33.35 dB, or 43.7 dB.cm³/g (with a measured density 0.7631 g cm⁻³), 4 times greater than that of traditional metal shielding materials (solid copper is 10 dB.cm³/g).²⁹ Theoretically, the total EMI effectiveness (SE_{total}) was recorded in terms of the contributions from reflection (SE_{R}) and absorbance (SE_{A}), that is, $SE_{\text{total}} = SE_{\text{R}} + SE_{\text{A}}$ (in dB). The effect of P3HT on SE_{R} is saturated upon reaching 35 wt%; however, the SE_{A} continues to decrease as the polymer content increases to 50 wt% (Fig. 4c, d). This results in a continuous reduction in SE_{total} of composite films with increasing P3HT contents. Apparently, the absorbance to the electromagnetic wave plays a dominant role in determining the SE_{total} of composite films. A similar phenomenon has been observed in the mesoporous carbon/fused silica composites.⁵

The versatility of the synergistic self-organization approach was demonstrated by extension to other material systems. Fig. 5 presents an example of rapid preparation of superhydrophobic films using P3HT and montmorillonite (MMT). The pristine MMT film is extremely hydrophilic, exhibiting a contact angle near 0°, see Fig. S13a.[†] However, the addition of 5 wt% P3HT is sufficient to transform a MMT film from superhydrophilic into hydrophobic (contact angle 122°, Fig. 5a). Upon increasing the P3HT content to 25 wt%, the surface roughness of the composite film was further increased (Fig. S13b[†]), producing a superhydrophobic surface (contact angle 161°, Fig. 5b,c). Similar to the GN composite films, MMT sheets likewise induced the heterogeneous nucleation of P3HT. Fig. 5e shows the XRD curves of the MMT powder, pristine P3HT and MMT-P3HT composite films, from which a markedly enhanced shoulder peak ($2\theta = 5.5^\circ$) as opposed to that of the pristine P3HT film is clearly visible. This indicates a more ordered crystal structure in MMT



composite films. The induction effect would arise from the fact that the addition of methanol strengthens the inter-chain interaction of P3HT and the interaction with MMT sheets, out of the need of minimizing the contact with non-solvent molecules. The improved MMT-P3HT interaction can also be observed in XPS. Fig. 5f presents the representative XPS result of the MMT composite film, where the S2P3 peak is discernable and can be deconvoluted into two peaks at 167.21 and 168.38 eV, respectively (Fig. 5g), indicating the higher binding energy between MMT platelets and P3HT chains.

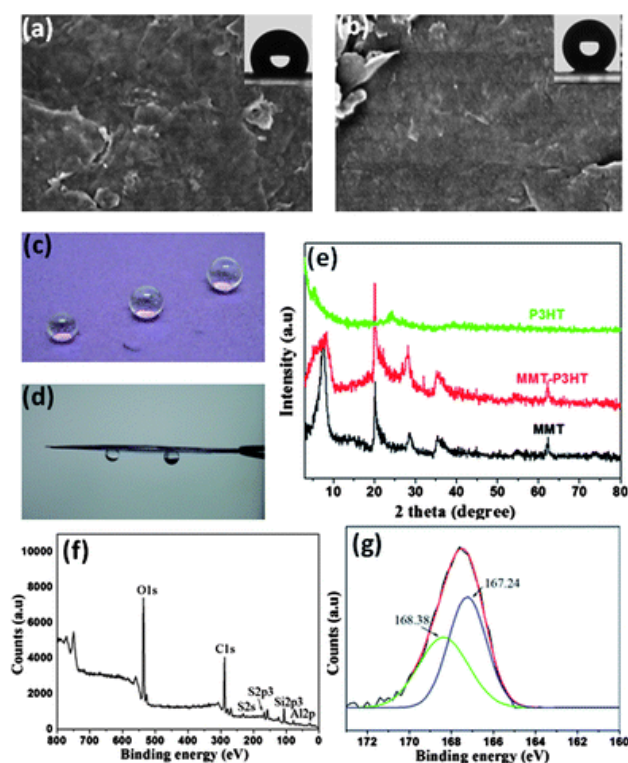


Fig. 5 SEM images of MMT composite films with 5 wt% P3HT (a) and 25 wt% P3HT (b); the insets show water contact angles of 122 and 161°, respectively. (c) Nearly spherical water droplets sit on the surface of a MMT composite film. (d) The strong adhesion capacity of the MMT composite film with 25 wt% P3HT. (e) XRD patterns of raw MMT powder, 25 wt% P3HT-MMT composite and pure P3HT films with a Cu-K α radiation $\lambda = 1.54 \text{ \AA}$ at 0.02°/s. (f) XPS results of the 25 wt% P3HT-MMT composite film. (g) XPS S2p3 core-level spectrum of the 25 wt% P3HT-MMT composite film shows strong interaction between P3HT and MMT.



However, unlike the GN composite film, the MMT composite film showed a high adhesion capacity to water droplets because of the contracted conformation of P3HT (Fig. 5c,d,S14), residual uncovered hydroxyl groups on the surface, and the capillary effect.

4. Conclusions

We have demonstrated a synergistic self-organization approach to produce superhydrophobic graphene composite films with attractive functionalities and environmental stability. The superhydrophobicity of composite films arises from the formation of multiscale rough surfaces; that is, nanoscale P3HT protrusions on the GN surface and microscale disordered stacking of GNs with protrusions. These protrusions effectively inhibit the close stacking of GNs during drying so that a lightweight, porous composite film with rough surfaces can be formed rapidly. Although our results were obtained from 2-dimensional nanoparticles (GN and MMT) and a conjugate polymer P3HT, it is completely possible to apply this approach to other nanoparticle-polymer systems, such as carbon nanotubes, metal (oxide) nanowires and non-conjugate polymers. This offers a technical advantage for rapid, economic industrial fabrication of a wide range of multifunctional film materials.

Acknowledgements: This work was supported by The National High Technology Research and Development Program of China (Grant No. 2008AA032102), NSF of China (Grant No. 50573014 and 50773012), and Shanghai Nanotechnology Program (Grant No. 1052nm00400).



References:

- 1 C. Cottin-Bizonne, J. L. Barrat, L. Bocquet and E. Charlaix, *Nat. Mater.*, 2003, 2, 237.
- 2 H. Y. Erbil, A. L. Demirel, Y. Avci and O. Mert, *Science*, 2003, 299, 1377.
- 3 R. Blossey, *Nat. Mater.*, 2003, 2, 301.
- 4 J. K. Yuan, X. G. Liu, O. Akbulut, J. Q. Hu, S. L. Suib, J. Kong and F. Stellacci, *Nat. Nanotechnol.*, 2008, 3, 332.
- 5 Y. M. Zheng, H. Bai, Z. B. Huang, X. L. Tian, F. Q. Nie, Y. Zhao, J. Zhai and L. Jiang, *Nature*, 2010, 463, 640.
- 6 J. Zhu, C. M. Hsu, Z. F. Yu, S. H. Fan and Y. Cui, *Nano Lett.*, 2010, 10, 1979.
- 7 F. Z. Zhang, L. L. Zhao, H. Y. Chen, S. L. Xu, D. G. Evans and X. Duan, *Angew. Chem., Int. Ed.*, 2008, 47, 2466.
- 8 O. Ikkala and G. ten Brinke, *Science*, 2002, 295, 2407.
- 9 H. S. Lee, S. M. Dellatore, W. M. Miller and P. B. Messersmith, *Science*, 2007, 318, 426.
- 10 A. Tuteja, W. J. Choi, M. L. Ma, J. M. Mabry, S. A. Mazzella, G. C. Rutledge, G. H. McKinley and R. E. Cohen, *Science*, 2007, 318, 1618.
- 11 J. Lahann, S. Mitragotri, T. N. Tran, H. Kaido, J. Sundaram, I. S. Choi, S. Hoffer, G. A. Somorjai and R. Langer, *Science*, 2003, 299, 371.
- 12 Y. Li, L. Li and J. Q. Sun, *Angew. Chem., Int. Ed.*, 2010, 49, 6129.
- 13 J. T. Han, S. Y. Kim, J. S. Woo and G. W. Lee, *Adv. Mater.*, 2008, 20, 3724.
- 14 C. Luo, X. L. Zuo, L. Wang, F. G. Wang, S. P. Song, J. Wang, J. Wang, C. H. Fan and Y. Cao, *Nano Lett.*, 2008, 8, 4454.
- 15 K. Koch, B. Bhushan and W. Barthlott, *Prog. Mater. Sci.*, 2009, 54, 137.
- 16 X. Zhang, F. Shi, J. Niu, Y. G. Jiang and Z. Q. Wang, *J. Mater. Chem.*, 2008, 18, 621.
- 17 (a) M. J. Liu, Y. M. Zheng, J. Zhai and L. Jiang, *Acc. Chem. Res.*, 2010, 43, 368; (b) K. S. Liu, X. Yao and L. Jiang, *Chem. Soc. Rev.*, 2010, 39, 3240–3255.
- 18 A. K. Geim, *Science*, 2009, 324, 1530.
- 19 F. Schwierz, *Nat. Nanotechnol.*, 2010, 5, 487.
- 20 Y. W. Zhu, S. Murali, M. D. Stoller, K. J. Ganesh, W. W. Cai, P. J. Ferreira, A. Pirkle, R. M. Wallace, K. A. Cychoz, M. Thommes, D. Su, E. A. Stach and R. S. Ruoff, *Science*, 2011, 332, 1537.
- 21 (a) S. Stankovich, D. A. Dikin, G. H. B. Dommett, K. M. Kohlhaas, E. J. Zimney, E. A. Stach, R. D. Piner, S. T. Nguyen and R. S. Ruoff, *Nature*, 2006, 442, 282; (b) X. L. Li and H. J. Dai, et al., *Nat. Nanotechnol.*, 2008, 3, 538; (c) R. D. McCullough, R. D. Lowe, M. Jayaraman and D. L. Anderson, *J. Org. Chem.*, 1993, 58, 904.
- 22 M. Fang, K. G. Wang, H. B. Lu, Y. L. Yang and S. Nutt, *J. Mater. Chem.*, 2009, 19, 7098.
- 23 M. Fang, K. G. Wang, H. B. Lu, Y. L. Yang and S. Nutt, *J. Mater. Chem.*, 2010, 20, 1982.
- 24 M. Fang, Z. Zhang, J. F. Li, H. D. Zhang, H. B. Lu and Y. L. Yang, *J. Mater. Chem.*, 2010, 20, 9635.
- 25 A. Nish, J. Y. Hwang, J. Doig and R. J. Nicholas, *Nat. Nanotechnol.*, 2007, 2, 640.
- 26 T. Yamamoto, D. Komarudin, M. Arai, B. L. Lee, H. Suganuma, N. Asakawa, Y. Inoue, K. Kubota, S. Sasaki, T. Fukuda and H. Matsuda, *J. Am. Chem. Soc.*, 1998, 120, 2047.
- 27 N. Kiriy, E. Jahne, H. J. Adler, M. Schneider, A. Kiriy, G. Gorodyska, S. Minko, D. Jehnichen, P. Simon, A. A. Fokin and M. Stamm, *Nano Lett.*, 2003, 3, 707.



28 T. Kashiwagi, F. M. Du, J. F. Douglas, K. I. Winey, R. H. Harris Jr and J. R. Shields, *Nat. Mater.*, 2005, 4, 928.

29 Y. L. Yang, M. C. Gupta, K. L. Dudley and R. W. Lawrence, *Nano Lett.*, 2005, 5, 2131.